

Theory of resonant inelastic X-ray scattering in vanadium oxides: how to detect $d-d$ excitations?

V. Yushankhai^{1,2} and L. Siurakshina^{1,2}

¹*Joint Institute for Nuclear Research,
141980 Dubna, Russia*

²*Max-Planck-Institut für Physik Komplexer Systeme,
Nöthnitzer Straße 38,
D-01187 Dresden, Germany*

(Dated: March 8, 2021)

Abstract

Generic low-energy spectral features related to $d-d$ excitations in nearly cubic vanadium perovskites are predicted for the expected L -edge resonant inelastic X-ray scattering (RIXS) measurements. Model Hamiltonian describing local electronic properties, including crystal-field effects, of vanadium $3d$ orbitals in the basic t_{2g}^2 configuration is formulated with the help of complementary *ab initio* quantum-chemical cluster calculations. In the presence of $2p$ -core hole, the local Hamiltonian includes strong $2p-3d$ electron interactions. As a prerequisite for evaluating RIXS transition amplitudes beyond the fast collision approximation, a symmetry-group approach is applied to generate a basis set of many-electron wavefunctions of the intermediate core-hole states accessible in RIXS processes. Although a comprehensive description of the core-hole multiplets still remains a formidable task and requires using specially designed numerical codes, for particular resonant states the analysis is simplified and the calculation of RIXS amplitude can be carried out analytically to the end.

I. INTRODUCTION

Soft X-ray resonant inelastic scattering (RIXS) is increasingly important in the study of electronic properties of strongly correlated $3d$ systems.¹ Measurements of $d-d$ excitations that correspond to local rearrangements of $3d$ electrons provide a valuable piece of information on the strong coupling between spin, orbital and lattice degrees of freedom in a system. Last years, the advances achieved on the instrumental side of RIXS make it possible to measure electronic excitations with energy resolution better than 0.1eV and, hence, to resolve fine features of electronic structure not accessible previously.

The family of vanadium oxides RVO_3 (with $R=Y$ or trivalent rare earth ion) with t_{2g}^2 configuration of V^{3+} ions have attracted much attention because of its rich and complex behavior.²⁻⁴ In these Mott-Hubbard insulating materials with a weak deviation from the ideal cubic perovskite structure the anticipated crystal-field (CF) splitting of t_{2g} orbitals is rather small $\sim 0.1\text{eV}$ and varies with structural changes. In these circumstances, to describe the low-energy properties of RVO_3 the orbital and spin degrees of freedom have to be treated on equal footing, which leads to a spin-orbital superexchange lattice model derived and studied in a series of papers.⁵⁻⁸ The model was shown to predict diverse behavior of the system in dependence on the model parameter chosen and complementary theoretical assumptions made. One of the basic assumptions concerns the choice of a point symmetry at V ion, the CF parameters and their variation along the RVO_3 series irrespective of any orbital and spin ordering. We note that CF splitting of t_{2g} orbitals and the multiplet structure of t_{2g}^2 configuration of V ion can be directly inferred from the low-energy part of high-resolution RIXS spectra provided the spectral features associated with $d-d$ excitations are properly identified as bound excitonic states, i.e., the low-energy in-gap electronic excitations produced by RIXS at the final stage in an insulating strongly correlated system.

In the present study, we examine theoretically the spectrum of $d-d$ excitations with special attention to a spin and orbital disordered phase of RVO_3 . In Sec.II, we begin with a brief description of several basic properties of nearly cubic vanadium perovskites, including the calculated electronic multiplet structure of the V^{3+} ion related to the expected RIXS spectra. Fundamentals of the vanadium L -edge ($2p-3d$ core-hole excitation) RIXS transitions are discussed in Sec.III. Since a comprehensive analysis of relevant RIXS transitions requires knowledge of intermediate core-hole states, this item is considered in Sec.IV in many detail.

A generic procedure for calculating the RIXS transition amplitudes together with a more detailed consideration of the lowest-energy $d-d$ excitation are present in Sec.V. Summary, conclusions, and outlook follow in Sec.VI.

II. VANADIUM OXIDES WITH NEARLY CUBIC PEROVSKITE STRUCTURE

At room temperature the crystal lattice of RVO_3 is described by an orthorhombic space group with the lattice constants $a \approx b \approx c/\sqrt{2}$. A relatively weak deviation from the ideal cubic structure is caused by a regular rotation, tilting and distortion of VO_6 octahedra. As a result, the cubic degeneracy of t_{2g} orbitals occupied by two electrons is removed and the accordingly weak CF splitting of $\sim 0.1\text{eV}$ is expected, which is controlled by a variation of the R-site ionic radius r_R along the RVO_3 series.

Interplay between weakly split t_{2g} orbitals, spins and lattice degrees of freedom is in the heart of a rich behavior observed in RVO_3 family, including two types of the orbital-ordering (OO) and spin-ordering (SO) patterns observed and reported in a number of works, as for instance, reviewed shortly in Ref.9. An ordering, called the C -OO, corresponds to the orbital arrangement of antiferro-type in ab -plane and ferro-type along the c -axis. The C -OO together with the antiferromagnetic G -type spin ordering (G -SO, with spins staggered in all three directions) occur at low temperatures, $T < 100\text{K}$, in RVO_3 with smallest r_R . The other ordering pattern is the G -OO accompanied with C -SO and observed at intermediate temperatures. The G -OO/ C -SO is the only ordered phase in RVO_3 with larger values of r_R . The global spin-orbital phase diagram for the RVO_3 family including the concomitant structural phase transitions derived from the single-crystal measurements was reported.^{2,9} Based on a spin-orbital superexchange model for RVO_3 a scenario of the puzzling transition between the two above-mentioned ordered phases was suggested.⁵⁻⁷

In the present paper, our main concern is to the local properties of vanadium valence $3d$ electrons. The local part $H_{loc} = H_{cf} + H_{d,C}$ of the underlying Hubbard-type model contains the crystal field H_{cf} and the Coulomb $H_{d,C}$ terms:

$$\mathcal{H}_{cf} = \sum_{m,\sigma} \epsilon_m^d d_{m\sigma}^\dagger d_{m\sigma},$$

$$H_{d,C} = U \sum_m n_{m\uparrow} n_{m\downarrow} + \sum_{m < m'} \left(U - \frac{5}{2} J_{mm'} \right) n_m n_{m'} - 2 \sum_{m \langle m'} J_{mm'} \mathbf{S}_m \mathbf{S}_{m'}$$

$$\sum_{m \neq m'} J_{mm'} d_{m\uparrow}^\dagger d_{m\downarrow}^\dagger d_{m'\downarrow} d_{m'\uparrow}. \quad (1)$$

Here, ϵ_m^d is an energy of the m -th $3d$ orbital, U and $J_{mm'}$ are the Hubbard repulsion and Hund's exchange parameters, respectively. When restricted only to the t_{2g} subspace, the Hamiltonian with the same exchange parameters, $J_{mm'} = J_H$, describes rigorously the multiplet structure of t_{2g}^2 and t_{2g}^3 configurations.^{5,10}

Because the octahedra VO_6 in RVO_3 are tilted and distorted, the exact point symmetry at V ion is rather low - the only operation allowed is the inversion, and the cubic $3d$ basis functions, t_{2g} and e_g , are generally mixed. Nevertheless, one expects that a higher point symmetry, for instance, D_{2h} or D_{4h} , can be applied to approximate accurately the CF levels and the electronic multiplet structure of the system. In support of this conjecture, we have performed complementary *ab initio* quantum-chemical calculations¹¹ for a crystal fragment containing the rotated and distorted cluster VO_6 . The calculated valence states are found to be hybridized V-ion $3d$ - and oxygen $2p$ -orbitals, and in a local orthogonal frame associated with the principal axes of a rotated octahedron these (antibonding) molecular orbitals can be viewed as the canonical t_{2g} and e_g ones. In the following, they are referred to as vanadium valence $3d$ orbitals, and the model Hamiltonian, Eq.(1), is applied to them as well. To estimate model parameters, energies of several crystal-field multiplets of the valence d^2 configuration, including t_{2g}^2 and $t_{2g}^1 e_g^1$, were calculated for the cluster VO_6 and compared with those derived from Eq.(1). We found that the expected for D_{4h} (or D_{2h}) point symmetry character of a comparatively weak non-cubic CF splitting, both within the t_{2g} and e_g subspaces, is well supported by the computed spectra, which is commented in detail below. Since the main focus is on the low-energy electronic properties and their measurements by RIXS, the calculated multiplet structure of the t_{2g}^2 configuration is mostly discussed.

To be more precise, we note that in the orthorhombic structure of RVO_3 there are four non-equivalent crystallographic positions of V-ions coordinated with oxygen octahedra that are rotated by the same angles in alternate manner. For a given V ion, assuming the x -, y -, and z -axes of the local coordinate system attached to the principal axes of the rotated oxygen octahedron, we define the t_{2g} orbitals as follows: $d_{yz} = d_\xi$, $d_{zx} = d_\eta$, and $d_{xy} = d_\zeta$. The angular part of the orbital wavefunctions are described by real spherical harmonics: $Z_\xi^2 = (i/\sqrt{2})[Y_{-1}^2 + Y_1^2]$, $Z_\eta^2 = (1/\sqrt{2})[Y_{-1}^2 - Y_1^2]$, and $Z_\zeta^2 = (i/\sqrt{2})[Y_{-2}^2 - Y_2^2]$, with Y_m^2 being

the canonical spherical harmonics.

In our *ab initio* quantum-chemical cluster approach based on the use of MOLPRO computer program¹², the wave functions and energies of electron configurations are calculated at different levels of accuracy - from a single-reference restricted Hartree-Fock (RHF) method through a multi-configuration self-consistent field (MCSCF) ansatz to the multi-reference configuration-interaction method (MRCI).¹³ The lattice fragment, whose electrons are treated rigorously, contains the cluster VO_6 and eight neighboring R ions, and it is imbedded in a large point-charge environment that simulates the Madelung potential on the cluster ions.

In our calculations the primary emphasis was placed upon the most widely studied compound YVO_3 . The structural lattice data with the actual rotation, tilting and distortion of VO_6 , reported⁴ for YVO_3 were used. Although the situation is likely to depend on the changing degree of octahedral tilting across the RVO_3 series¹⁴⁻¹⁶, we expect that the generic features derived can be directly extended to other members of the RVO_3 family, at least to those with close values of r_R . Therefore, keeping in mind such an extended usage of our cluster calculations, most representative results are reported throughout. As expected the calculated subspaces e_g and t_{2g} are well separated by a large cubic CF of $\sim 1.5\text{eV}$. For the high-temperature ($T > 200\text{K}$) orthorhombic structure the lowest electronic orbital is d_ζ , while the pair of d_η , d_ξ is shifted up by $\Delta_1 \sim 0.1\text{eV}$, and these two are only weakly split by $\Delta_2 \sim 10\text{meV}$. The inequality $\Delta_1 \gg \Delta_2$ can be partly explained for the high- T phase by the observation⁴ that in each oxygen octahedron the tetragonal-like contraction of the V-O bonds along z -axis is regularly larger than an orthorhombic distortion of the V-O bonds in the xy -plane. Because the energy resolution of RIXS spectra is usually limited to $\sim 50\text{meV}$, in the multiplet structure fine features due to orthorhombic CF level splitting of $\Delta_2 \sim 10\text{meV}$ can be hardly resolved. Therefore, in subsequent theoretical analysis of the local electronic structure characteristic of the high- T phase of RVO_3 , instead of D_{2h} we use the tetragonal D_{4h} symmetry by setting $\Delta_2 \rightarrow 0$ and denoting the largest non-cubic CF parameter for the t_{2g} manifold as $\Delta_1 = \Delta_t$. This is in contrast to the CF model suggested in Ref.6. There, the authors assumed the cubic point symmetry O_h with fully degenerate t_{2g} levels in the high- T phase and a symmetry reduction from O_h to D_{4h} (or D_{2h}) was associated with structural transitions below 200K.

In high- T phase of RVO_3 the low-energy part of the RIXS spectra is expected to exhibit

the multiplet structure of t_{2g}^2 configuration. Hereafter, a simplifying approximation is used that consists in the neglect of comparatively small alternating tilts of oxygen octahedra. Thus all the vanadium ions are considered to be equivalent and the $3d$ orbitals are defined in the global (XYZ) -coordinate system with Z -axis along the orthorhombic \mathbf{c} -axis, while X - and Y -axis are rotated by 45° with respect to \mathbf{a} and \mathbf{b} .

For the CF of D_{4h} symmetry, the states of t_{2g}^2 configuration are sorted over the terms 3E , 3A_2 , 1E , 1B_2 , 1B_1 , and $2\ {}^1A_1$, where a subscript indicating the same (even) parity of terms is omitted for brevity. For a given term ${}^{2S+1}\Gamma \equiv (S\Gamma)$, the basis functions $|t^2(S\Gamma)M\gamma\rangle$ labeled by the spin projection $M(= -S, -S + 1, \dots, S)$ and the basis index γ of Γ , form a set of degenerate eigenfunctions of the local Hamiltonian, Eq.(1). The calculated multiplet structure is presented schematically in Fig.1. The term energies are found to be: $\mathcal{E}({}^3A_2) = \Delta_t$, $\mathcal{E}({}^1A_1) = 2J_H - \Delta\mathcal{E}'$, $\mathcal{E}({}^1E) = 2J_H$, $\mathcal{E}({}^1B_1) = \mathcal{E}({}^1B_2) = \Delta_t + 2J_H$, $\mathcal{E}({}^1A_1) = 5J_H + \Delta\mathcal{E}'$, where $\Delta\mathcal{E}' \approx \Delta_t[1 + (\Delta_t/J_H)]/3$, for $\Delta_t/J_H < 1/2$, with the reference energy taken at the level of lowest term 3E of t_{2g}^2 configuration. From our cluster calculations, it follows also that, first, the lowest spin-triplet level coming from the $t_{2g}^1e_g^1$ configuration falls into the same energy range - it is stuffed between ${}^1B_1/{}^1B_2$ and 1A_1 , but not indicated in Fig.1. Second, the estimated value of Hund's constant is $J_H \approx 0.5\text{eV}$, which is somewhat smaller than that reported usually in literature.^{17,18}

For the further purposes, it is instructive to present explicitly the basis functions of several terms under consideration. For instance, the ground-state term 3E comprises six states: $|t^2({}^3E)Me_1\rangle = |d_{\eta\uparrow}d_{\zeta\uparrow}\rangle$, $(1/\sqrt{2})[|d_{\eta\uparrow}d_{\zeta\downarrow}\rangle + |d_{\eta\downarrow}d_{\zeta\uparrow}\rangle]$, $|d_{\eta\downarrow}d_{\zeta\downarrow}\rangle$, for $\gamma = e_1$, and the other three states $|t^2({}^3E)Me_2\rangle$ for $\gamma = e_2$ are obtained by the replacement $\eta \rightarrow \xi$. The first excited term is a triplet $|t^2({}^3A_2)M\rangle = |d_{\xi\uparrow}d_{\eta\uparrow}\rangle$, $(1/\sqrt{2})[|d_{\xi\uparrow}d_{\eta\downarrow}\rangle + |d_{\xi\downarrow}d_{\eta\uparrow}\rangle]$, $|d_{\xi\downarrow}d_{\eta\downarrow}\rangle$, where the basis index γ for the one-dimensional representation A_2 is omitted. In all sets above, states are listed according to $M = +1, 0, -1$. With respect to RIXS, the initial (ground) and excited (final) states are denoted below as $|t^2, [g]\rangle$ and $|t^2, [f]\rangle$, respectively. Here, $[g]$ and $[f]$ are the shortenings for the quantum numbers, $[g] = ({}^3E)M_g e_g$ with $M_g = 0, \pm 1$ and $e_g = e_{1,2}$, and $[f] = (S_f\Gamma_f)M_f\gamma_f$.

III. RIXS THEORY: BASIC FORMULATION

Consider a typical scheme of the L -edge RIXS measurement for a strongly correlated $3d$ -electron system whose N -electron ground state is $|\Psi_{[g]}^N\rangle$. The incoming photon with momentum $\hbar\mathbf{k}$ and energy $\hbar\omega_{\mathbf{k}}$ tuned close to the L -edge absorption promotes an electron from the $2p$ shell to an empty $3d$ valence state, thus producing an intermediate core-hole state $|(\Psi^{N+1}\underline{p})_{[i]}\rangle$. In a subsequent radiative decay of the core hole the emitted $(\hbar\mathbf{k}', \hbar\omega_{\mathbf{k}'})$ photon leaves the $3d$ electron system in an excited state $|\Psi_{[f]}^N\rangle$ with momentum $\hbar(\mathbf{k} - \mathbf{k}')$ and energy $\hbar(\omega_{\mathbf{k}} - \omega_{\mathbf{k}'})$ that are measured. For given polarization vectors $\boldsymbol{\epsilon}$ and $\boldsymbol{\epsilon}'$ of the incoming and outgoing photons, respectively, the scattering amplitude of the second-order resonant processes governed by the transition operator $\mathbf{D}_{\mathbf{k}}$ can be written¹ as

$$\mathcal{F}_{fg}^{\boldsymbol{\epsilon}'\boldsymbol{\epsilon}}(\mathbf{k}', \mathbf{k}; z_{\mathbf{k}}) = \langle \Phi_{[f]}^N | (\boldsymbol{\epsilon}' \mathbf{D}_{\mathbf{k}'})^\dagger \mathcal{G}(z_{\mathbf{k}}) (\boldsymbol{\epsilon} \mathbf{D}_{\mathbf{k}}) | \Phi_{[g]}^N \rangle. \quad (2)$$

Here, $\mathcal{G}(z_{\mathbf{k}})$ is the intermediate-state propagator which describes the system in the presence of a core hole:

$$\mathcal{G}(z_{\mathbf{k}}) = \sum_{\{i\}} \frac{|(\Phi^{N+1}\underline{p})_{[i]}\rangle \langle (\Phi^{N+1}\underline{p})_{[i]}|}{z_{\mathbf{k}} - E_{[i]}}, \quad (3)$$

where $z_{\mathbf{k}} = \hbar\omega_{\mathbf{k}} + i\Gamma$, for $E_{[g]} = 0$, and the lifetime broadening Γ of intermediate core-hole states is taken to be independent on the state index $[i]$. We note that Γ depends on the $3d$ -ion species probed in a measurement and, typically, ranges^{19,20} from 0.2eV up to 0.6eV. In the dipole limit, the transition operator $\mathbf{D}_{\mathbf{k}}$ takes the form

$$\mathbf{D}_{\mathbf{k}} = \frac{1}{\mathcal{N}} \sum_l e^{i\mathbf{k}\mathbf{R}_l} \sum_{j(l)}^{N_e} (\mathbf{r}_j - \mathbf{R}_l), \quad (4)$$

where \mathbf{R}_l denotes the lattice sites of the metal ions and the second summation is over electrons belonging to the l -th ion. The form Eq.(4) is especially suitable since we are mainly interested in the bound excitonic states, i.e., the low-energy in-gap electronic excitations produced by RIXS at the final stage in an insulating strongly correlated system.

Then, in the second-quantization form the dipole operator Eq.(4) reads ($\mathbf{R}_l \equiv \mathbf{l}$):

$$\mathbf{D}_{\mathbf{k}} = \frac{\mathcal{R}^2}{\mathcal{N}} \sum_{\mathbf{l}} e^{i\mathbf{k}\mathbf{l}} \left(\sum_{m,\sigma} \sum_{m_p} \langle Z_m^2 | \hat{\mathbf{r}} | Y_{m_p}^1 \rangle d_{l m \sigma}^\dagger p_{l m_p \sigma} + H.c. \right). \quad (5)$$

Here the operator $p_{l m_p \sigma}$ destroys an electron with the orbital projection $m_p (= 0, \pm 1)$ and spin σ in the $2p$ shell, while $d_{l m \sigma}^\dagger$ creates an extra electron with the same spin in the m -th orbital

of the $3d$ -shell, $\hat{\mathbf{r}} = \mathbf{r}/|\mathbf{r}|$, and \mathcal{R}^2 contains an integral over radial $2p$ and $3d$ wavefunctions. One may check that $\mathbf{D}_{\mathbf{k}}^\dagger = \mathbf{D}_{-\mathbf{k}}$. At this stage, a strong $2p$ spin-orbit coupling can be taken into account by the following replacement

$$p_{1m_p\sigma} = \sum_{j,m_j} C_{1m_p\frac{1}{2}\sigma}^{jm_j} p_{1jm_j}, \quad (6)$$

where $C_{1m_p\frac{1}{2}\sigma}^{jm_j}$ are Clebsch-Gordan coefficients for an electron with a total angular momentum $j = 3/2, 1/2$. The insertion of Eq.(6) into Eq.(5) splits the dipole operator: $\mathbf{D}_{\mathbf{k}} = \mathbf{D}_{\mathbf{k}}(j = 3/2) + \mathbf{D}_{\mathbf{k}}(j = 1/2)$. Below we focus on the L_3 -edge scattering processes only and, therefore, in Eq.(6) the sum is bounded to $m_j = \pm 3/2, \pm 1/2$, for $j = 3/2$.

By applying the circular components $q (= 0, \pm 1)$ to vectors $\boldsymbol{\epsilon}$ and $\hat{\mathbf{r}}$, the scattering amplitude Eq.(2) can be rewritten as

$$\mathcal{F}_{fg}^{\boldsymbol{\epsilon}'\boldsymbol{\epsilon}}(\mathbf{k}', \mathbf{k}; z_k) = \sum_{q',q} T_{q'q}(\boldsymbol{\epsilon}', \boldsymbol{\epsilon}) F_{q'q}(g \rightarrow f; z_k), \quad (7)$$

where $T_{q'q}(\boldsymbol{\epsilon}', \boldsymbol{\epsilon}) = (-1)^{q'+q} \epsilon'_{-q'} \epsilon_{-q}$ is the polarization tensor and $F_{q'q}(g \rightarrow f; z_k)$ is called the partial amplitude.¹

From Eqs.(2),(5), and (7) one may see that a scattering process being considered as the sequence of two local dipole transitions is modulated in space by the phase factor $\exp[i(\mathbf{k} - \mathbf{k}')\cdot \mathbf{l}]$, which makes it possible to measure, besides the local d - d excitation, the dispersion laws of accessible propagating electronic excitations.¹ These include spin and orbital waves, and their mixture in spin-orbital ordered phases, as well as delocalized excitonic states whose propagation may be largely influenced by spin and orbital degrees of freedom. Nevertheless, an analysis of the in-gap excitation spectra, together with the corresponding transition probabilities and polarization dependence, has to be started with a calculation of a generic local dipole transitions.

The frequently used fast collision approximation^{1,21-23} may considerably simplify a theoretical analysis of RIXS processes. In general outline, instead of taking proper account of the individual scattering events that connect the ground state $|\Psi_{[g]}^N\rangle$ to a given final state $|\Psi_{[f]}^N\rangle$ through the intermediary of core-hole states, in this approximation one simply applies an averaging procedure that consists in the replacement of the intermediate-state propagator by a resonance factor $G(z_{\mathbf{k}}) \rightarrow (z_{\mathbf{k}} - \bar{\Omega}_{res})^{-1}$. Such an approximation could be well justified if, for instance, the lifetime broadening Γ of the intermediate core-hole states probed

is comparatively large, which is not the case in vanadium oxides where $\Gamma \approx 0.3\text{eV}$ is much smaller than the intermediate-state interactions.

To go beyond the fast collision approximation one has to take into account the multiplet structure of the intermediate core-hole states explicitly. The problem is extremely complicated by the fact that in the transition metal ions involved (i.e., V ions) the intra-atomic $2p$ - $3d$ interactions are strong, or more precisely, the Coulomb and exchange $2p$ - $3d$ integrals are of the same order as those for the valence $3d$ orbitals. As known, the multiplet structure of core-hole states is directly measured by the X-ray absorption spectroscopy (XAS). Nowadays, XAS spectra for strongly correlated electronic systems are usually predicted and/or the measured spectra are interpreted with the use of specially designed computer programs.²⁴⁻²⁸

In principle, the computer code for quantum-chemical cluster calculations we used for calculating the multiplet structure of d^2 configuration of V^{3+} ion (Section II), can be extended and applied for solving the core-hole multiplets as well. Nevertheless, it is tempting first to apply the symmetry-group technique and determine the intermediate-state many-electron wavefunctions of interest, and then proceed to the calculation of RIXS amplitudes without using complementary numerical procedures - the goal that is pursued in the following discussion.

IV. INTERMEDIATE CORE-HOLE STATES IN RVO_3

The first apparent aim is to calculate the on-site matrix elements (site index \mathbf{l} is omitted): $\langle (d^{N+1}\underline{p})_{[i]} | d_{m\sigma}^\dagger p_{\frac{3}{2}m_j} | d_{[g]}^N \rangle$ and $\langle d_{[f]}^N | p_{\frac{3}{2}m_j}^\dagger d_{m'\sigma'} | (d^{N+1}\underline{p})_{[i]} \rangle$, which involve two-electron states $|d_{[g]/[f]}^{N=2}\rangle$ of the low-energy configuration t_{2g}^2 discussed in Section II. The intermediate states $| (d^{N+1}\underline{p})_{[i]} \rangle$ containing one more electron in $3d$ valence shell and a core hole in $2p$ shell have to be determined as eigenvectors of the local Hamiltonian H_{loc} extended by including the $2p$ - $3d$ interactions $H_{pd,CX}$ and the spin-orbit coupling $H_{p,so}$ of $2p$ electrons

$$H_{loc} = H_{cf} + H_{d,C} + H_{pd,CX} + H_{p,so}. \quad (8)$$

The strength of the direct Coulomb (C) and the exchange (X) interactions entering the Hamiltonian $H_{pd,CX}$ are parametrized with the Slater integrals F_{pd}^0 , F_{pd}^2 , and G_{pd}^1 , G_{pd}^3 , respectively. For the $3d^3 2p^5 = (d^3 \underline{p})$ configuration of V ion, representative values²⁹ are: $F_{pd}^2 \approx 6\text{eV}$, $G_{pd}^1 \approx 4.4\text{eV}$ and $G_{pd}^3 \approx 2.5\text{eV}$. The monopole integral F_{pd}^0 provides a common

shift of all the multiplets under consideration.

To consider the full multiplet structure of the intermediate core-hole states, an appropriate basis set is build up in few steps. First, we define the auxiliary states $|d^3(S_1\Gamma_1)M_1\gamma_1\rangle$ of the d^3 configuration not disturbed by $H_{pd,CX}$. Similar to the d^2 configuration, this is done by specifying a set of terms $(S_1\Gamma_1)$, each composed of degenerate eigenstates of $H_{cf} + H_{d,C}$ with the corresponding eigenvalues $\mathcal{E}_d(S_1\Gamma_1)$. At this step, the approximation can be used that consists in the neglect in H_{cf} of a weak tetragonal distortion $\Delta \sim 0.1\text{eV}$ compared to a strong cubic CF component $\approx 1.5\text{eV}$. Regarding the intermediate states available in RIXS processes, this approximation is justified as follows: Like in X-ray absorption, any CF distortion, as well as a many-body interaction, that causes small energy effects compared to the lifetime broadening Γ ($\approx 0.3\text{eV}$ for vanadates) cannot be resolved. Loosely speaking, the fast collision approximation can be safely applied separately to each narrow group of (quasi-)degenerate intermediate states, but not to the total set of states.

In case of cubic CF symmetry, the t_{2g}^3 configuration is given by four $(S_1\Gamma_1)$ terms, namely, 4A_2 , 2E , 2T_1 , and 2T_2 , with the lowest 4A_2 and degenerate 2E and 2T_1 . With the reference to the lowest level $\mathcal{E}_d(^4A_2)$, the term positions are $\mathcal{E}_d(^2E) = \mathcal{E}_d(^2T_1) = 3J_H$ and $\mathcal{E}_d(^2T_2) = 5J_H$. For the further purposes, four spin states of 4A_2 deserve to be presented explicitly (the sole γ is omitted):

$$\begin{aligned}
|t^3(^4A_2), M_1 = 3/2\rangle &= |d_{\xi\uparrow}d_{\eta\uparrow}d_{\zeta\uparrow}\rangle, \\
|t^3(^4A_2), M_1 = 1/2\rangle &= \frac{1}{\sqrt{3}}(|d_{\xi\uparrow}d_{\eta\uparrow}d_{\zeta\downarrow}\rangle + |d_{\xi\uparrow}d_{\eta\downarrow}d_{\zeta\uparrow}\rangle + |d_{\xi\downarrow}d_{\eta\uparrow}d_{\zeta\uparrow}\rangle), \\
|t^3(^4A_2), M_1 = -1/2\rangle &= \frac{1}{\sqrt{3}}(|d_{\xi\downarrow}d_{\eta\downarrow}d_{\zeta\uparrow}\rangle + |d_{\xi\downarrow}d_{\eta\uparrow}d_{\zeta\downarrow}\rangle + |d_{\xi\uparrow}d_{\eta\downarrow}d_{\zeta\downarrow}\rangle), \\
|t^3(^4A_2), M_1 = -3/2\rangle &= |d_{\xi\downarrow}d_{\eta\downarrow}d_{\zeta\downarrow}\rangle.
\end{aligned} \tag{9}$$

The states contained in other terms $(S_1\Gamma_1)$ can be presented in a similar manner as well.

Vector coupling of two irreducible representations S_1 and Γ_1 leads to an equivalent description of the t_{2g}^3 configuration in terms of representations $\bar{\Gamma}$ with the corresponding states

$$|t^3, \bar{\Gamma}\bar{\gamma}(S_1\Gamma_1)\rangle = \sum_{M_1, \gamma_1} |t^3(S_1\Gamma_1)M_1\gamma_1\rangle U_{M_1\gamma_1, \bar{\Gamma}}^{S_1\Gamma_1, \bar{\Gamma}}, \tag{10}$$

where coefficients $U_{M_1, \gamma_1, \bar{\Gamma}}^{S_1\Gamma_1, \bar{\Gamma}}$ of the unitary transformation, Eq. (10), are tabulated³⁰ (both for the single and double-valued point groups). Next we note that for the $2p$ core-hole with total angular momentum $j = 3/2$, the states $|p_{\frac{3}{2}m_j}\rangle$ transform according to the four-dimensional

double-valued representation $G_{3/2}$ (Γ_8 in the Bethe system) of the cubic group, and the notation $|\underline{p}_{\frac{3}{2}m_j}\rangle = |\underline{p}, G_{3/2}m_j\rangle$, with $m_j = \pm 3/2, \pm 1/2$, is more convenient.

Finally, the complete basis set $|t^3\underline{p}, \Gamma_J\gamma_J\rangle$ for the core-hole configuration $t^3\underline{p}$ is determined by vector coupling of the representations $\bar{\Gamma}$ for the "undisturbed" valence t_{2g}^3 configuration, Eq. (10), and $G_{3/2}$ for the $2p$ core hole. The coupling relation reads

$$|t^3\underline{p}, \Gamma_J\gamma_J(\bar{\Gamma}G_{3/2})(S_1\Gamma_1)\rangle = \sum_{\bar{\gamma}, m_j} |t^3, \bar{\Gamma}\bar{\gamma}(S_1\Gamma_1)\rangle |\underline{p}, G_{3/2}m_j\rangle U_{\bar{\gamma}m_j, \gamma_J}^{\bar{\Gamma}G_{3/2}, \Gamma_J}, \quad (11)$$

with the coupling coefficients $U_{\bar{\gamma}m_j, \gamma_J}^{\bar{\Gamma}G_{3/2}, \Gamma_J}$ defined as in Ref.30. In general, when the procedure outlined above is applied, several repeating representations $\Gamma_J, \Gamma'_J, \Gamma''_J$, etc., of the same dimensionality may be generated. Repeating representations are discriminated with additional labeling, $(S_1\Gamma_1)$ and $(\bar{\Gamma}G_{3/2})$, kept in Eq.(11), to indicate different routes $(S_1\Gamma_1) \rightarrow (\bar{\Gamma}G_{3/2}) \rightarrow \Gamma_J$ the representations Γ_J or Γ'_J, Γ''_J arise. Below we refer to $(S_1\Gamma_1)$ as the generating multiplet.

Eq.(11) suggests a conventional basis for a diagonalization of the local Hamiltonian, Eq.(8). Insofar as states of repeating representations are mixed by $H_{pd,CX}$, the matrix of H_{loc} takes a block-diagonal form, which can be solved numerically to give the full multiplet structure of the core-hole configuration $t^3\underline{p}$. Here, the main difficulty stems from the fact that complicated vector-coupled functions, Eqs.(10) and (11), come into play and calculation of numerous off-diagonal matrix elements of H_{loc} becomes very tedious. Nevertheless, close analysis shows that in several cases calculations are greatly simplified and some prominent features of the multiplet structure of a core-hole configuration can be evaluated without dealing with the full form of high-rank matrices of H_{loc} . A particular example is considered in the next Section.

V. RIXS TRANSITIONS IN RVO₃

Let us first apply the outlined procedure for examining the states of those Γ_J 's that are related to the lowest generating term $(S_1\Gamma_1)=^4A_2$. Because A_2 is one-dimensional representation, the Eq.(10) allows the following identification

$$|t^3, \bar{\Gamma}\bar{\gamma}(^4A_2)\rangle = |t^3, \bar{\Gamma} = G_{3/2}, \bar{\gamma} = M_1(^4A_2)\rangle \equiv |t^3(^4A_2), M_1\rangle, \quad (12)$$

with the final kets defined in Eq.(9). Then, according to Eq.(11), all irreducible representations Γ_J 's generated from the term 4A_2 are contained in the direct group product $G_{3/2} \otimes G_{3/2}$

and given³⁰ in the following decomposition: $G_{3/2} \otimes G_{3/2} = A_1 + A_2 + E + T_1 + T'_1 + T_2 + T'_2$. Without $2p$ - $3d$ interactions the terms are degenerate, however, being subjected to $H_{pd,CX}$ they are split into two subsets in such a way that each subset is coupled by $H_{pd,CX}$ to states of other multiplets in different manners. To exhibit this splitting, the term energies are preliminary found to the first order in $H_{pd,CX}$ by calculating the corresponding diagonal matrix elements of the local Hamiltonian, Eq.(8). This yields three lowest terms, A_2 , T_1 and T_2 , residing at the same energy that is taken below as the reference (zero) level. Then, the other four terms are shifted to higher energies as follows: A_1 at $\frac{8}{15}G_{pd}^1 + \frac{12}{35}G_{pd}^3$, E and T'_2 at $\frac{4}{15}G_{pd}^1 + \frac{6}{35}G_{pd}^3$, and T'_1 at $\frac{17}{30}G_{pd}^1 + \frac{2}{7}G_{pd}^3$.

The states of three lowest terms, A_2 , T_1 and T_2 , the first subset, can be regarded as "edge" resonant states for several reasons. Firstly, to any order in $H_{pd,CX}$ the "edge" states are not mixed with other states of the $t^3\underline{p}$ configuration - the corresponding off-diagonal matrix elements of H_{loc} are checked to be zero. To the contrary, the second subset, i.e., the states of complementary multiplets A_1 , E , T'_2 and T'_1 , are mixed up with states $|t^3\underline{p}, \Gamma_J\gamma_J(S_1\Gamma_1)\rangle$ of similar multiplets generated from $(S_1\Gamma_1) \neq^4A_2$ and located well above the reference level. In total, this mixture gives rise to a broad and dense manifold of intermediate states $|t^3\underline{p}, \Gamma_J\gamma_J\rangle$, but still the energy of "edge" states is retained below the bottom of this broad manifold. The "edge" states are stabilized mainly due to, first, that the initial energy of the generating term 4A_2 is well below the positions of other terms $(S_1\Gamma_1) \neq^4A_2$ and, second, for $\Gamma_J = A_2$, T_1 and T_2 the exchange coupling of the valence states $|t^3, M_1(^4A_2)\rangle$ to the core states $|\underline{p}, G_{3/2}m_j\rangle$ due to $H_{pd,CX}$ is optimized. Experimentally, concerning the L_3 -edge XAS/RIXS measurements in RVO_3 , the "edge" states should be associated with the lowest peak expected at the very edge of the XAS absorption spectra, while in RIXS they are accessible by tuning the incident photons to the lowest resonance energy $\Omega_{res}^{(1)}$, i.e., as $\hbar\omega_{\mathbf{k}} \rightarrow \Omega_{res}^{(1)}$.

Thus emerging multiplet structure of the core-hole configuration $t^3\underline{p}$ suggests that close to the "edge"-states associated with the resonance at $\Omega_{res}^{(1)}$, the remaining terms Γ_J evolve into a peak-shaped structure of several features at higher energies, $\Omega_{res}^{(n)} > \Omega_{res}^{(1)}$, for $n = 2, 3, \dots$. Particular peaks initially assigned to different Γ_J 's are broadened due the core-hole lifetime effects. A group of peaks may overlap if their energy spacing is less than the core-hole lifetime broadening. This means that a set of core-hole states $|t^3\underline{p}, \Gamma_J\gamma_J\rangle$ that are included in a group of "closely spaced" Γ_J 's, are not resolved and should be attributed to a peculiar resonance energy $\Omega_{res}^{(n)}$, which is denoted below as $\{\Gamma_J\gamma_J\} \in (n)$. Then the partial amplitude

of corresponding local transitions can be expressed in the following form

$$F_{q'q}(g \rightarrow f; \Omega_{res}^{(n)}) = \sum_{\{\Gamma_J \gamma_J\} \in (n)} \frac{\langle t^2, [f] | \overline{\mathcal{D}}_q | t^3 \underline{p}, \Gamma_J \gamma_J \rangle \langle t^3 \underline{p}, \Gamma_J \gamma_J | \mathcal{D}_q | t^2, [g] \rangle}{z_k - \hbar \Omega_{res}^{(n)}}, \quad (13)$$

where \mathcal{D}_q is the q -th component of the dipole operator, Eq.(5), taken at $\mathbf{k} = 0$. Eq.(13) shows that the states involved in $\{\Gamma_J \gamma_J\} \in (n)$ interfere to yield a joint transition at the resonance energy $\hbar \Omega_{res}^{(n)}$.

To predict the relative positions of $\Omega_{res}^{(n)}$, the eigenvalue problem should be solved by diagonalizing numerically the local Hamiltonian, Eq.(8), with the basis set defined in Eq.(11). Together with the calculated eigenstates $|t^3 \underline{p}; \Gamma_J \gamma_J\rangle$, this would give one a firm ground for a comprehensive account of RIXS transition probabilities. As mentioned above, instead of performing this ambitious program, here we focus on solving a restricted problem - calculation of the RIXS transitions that occur via the resonant "edge" states, which can be accomplished analytically to the end.

The explicit form of "edge" states follows directly from Eqs.(10) and (11). In Eq.(11) the coupling coefficients $U_{\gamma m_j, \gamma_J}^{\overline{\Gamma} G_{3/2}, \Gamma_J}$ required for $\overline{\Gamma} = G_{3/2}$ and $\Gamma_J = A_2, T_1$ and T_2 , are found from tables of Ref.30. For the sake of brevity, we reduce slightly the notation as follows: $U_{M_1 m_j, \gamma_J}^{G_{3/2} G_{3/2}, \Gamma_J} \equiv \mathcal{U}_{M_1 m_j}^{\Gamma_J \gamma_J}$. Complementary reduction includes both $|\underline{p}, G_{3/2} m_j\rangle = |\underline{p}, m_j\rangle$, where $m_j = \pm 3/2, \pm 1/2$ for the core-hole states, and $|t^3 \underline{p}; \Gamma_J \gamma_J (G_{3/2} G_{3/2}) (^4 A_2)\rangle = |t^3 \underline{p}; \Gamma_J \gamma_J\rangle$ for the "edge"-state kets. In shortened notations the latter can be now expressed as

$$|t^3 \underline{p}, \Gamma_J \gamma_J\rangle = \sum_{M_1, m_j} |t^3, (^4 A_2) M_1\rangle |\underline{p}, m_j\rangle \mathcal{U}_{M_1 m_j}^{\Gamma_J \gamma_J}, \quad (14)$$

where the kets $|t^3, (^4 A_2) M_1\rangle$ are defined in Eq.(9).

As $\omega_{\mathbf{k}} \rightarrow \Omega_{res}^{(1)}$, the local RIXS transitions are described by partial amplitude, Eq.(13), where $\{\Gamma_J \gamma_J\} \in (1)$ denotes the lowest energy degenerate multiplets $\Gamma_J = A_2, T_1$ and T_2 of the $t^3 \underline{p}$ configuration. Matrix elements of the dipole operator are given by

$$\langle t^2, [f] | \overline{\mathcal{D}}_q | t^3 \underline{p}, \Gamma_J \gamma_J \rangle = \mathcal{R}^2 \sum_{M_1, \sigma} \sum_{m, m_p} \langle t^2, [f] | d_{m\sigma} | t^3, M_1 \rangle \left[\sum_{m_j} \mathcal{U}_{M_1 m_j}^{\Gamma_J \gamma_J} C_{1 m_p \frac{1}{2} \sigma}^{3/2 m_j} \right] \langle Y_{m_p}^1 | \hat{r}_q | Z_m^2 \rangle, \quad (15)$$

The complex conjugate of Eq.(15) and the replacement $q' \rightarrow q, [f] \rightarrow [g]$ then yields $\langle t^3 \underline{p}, \Gamma_J \gamma_J | \mathcal{D}_q | t^2, [g] \rangle$. Having the states $|t^2, [f]/[g]\rangle$ and $|t^3, M_1\rangle$ as defined in Section II and Eq.(9), together with the symmetry coupling $\mathcal{U}_{M_1 m_j}^{\Gamma_J \gamma_J}$ and Clebsch-Gordan $C_{1 m_p \frac{1}{2} \sigma}^{3/2 m_j}$ coefficients known, the transition amplitudes at $\hbar \omega_{\mathbf{k}} \rightarrow \Omega_{res}^{(1)}$ are calculated straightforwardly.

A connection of the ground state $|t^2, [g]\rangle$ to particular final states $|t^2, [f]\rangle$ depicted in Fig.1 and a polarization dependence of the transitions are of the main interest.

The calculations show that besides the elastic transition, $|t^2, ({}^3E)M_g e_g\rangle \rightarrow |t^2, ({}^3E)M'_g e'_g\rangle$, the only excited term of t_{2g}^2 configuration accessible via the resonance at $\Omega_{res}^{(1)}$ is 3A_2 , Fig.1. This occurs in the processes $|t^2, ({}^3E)M_g e_g\rangle \rightarrow |t^2, ({}^3A_2)M_f\rangle$ with the initial and final states being degenerate in $M_g(= 0, \pm 1)$, $e_g(= e_1, e_2)$ and $M_f(= 0, \pm 1)$, respectively, for the disordered high- T phase. As seen from Fig.1, the corresponding excitation energy is $\hbar\omega_{fg} = \Delta_t$, and thus the basic CF parameter can be measured directly together with a fully identified excitonic state. A possible band broadening of this excitonic state is discussed later on. Identification of this peculiar $d-d$ transition in RIXS measurements of RVO_3 would enhance a better understanding of the system. For instance, a trend of interest that Δ_t develops upon replacement of R ion in RVO_3 can be followed. Second, from Eqs.(13),(15) one obtains the transition intensity

$$\mathcal{I}^{\epsilon'\epsilon}(\omega_{fg} \simeq \Delta_t, \Omega_{res}^{(1)}) = \mathcal{A} \sum_{M_f} \sum_{M_g, e_g} \sum_{q', q} |T_{q'q}(\epsilon', \epsilon) F_{q'q}({}^3E)M_g e_g \rightarrow ({}^3A_2)M_f; \Omega_{res}^{(1)}|^2, (16)$$

where \mathcal{A} is the known constant.¹ Note that in Eq.(16) an averaging over the initial states and summation over the final states are performed assuming the state degeneracy mentioned. From this, the calculated polarization dependence is given up to a factor as

$$\mathcal{I}^{\epsilon'\epsilon}(\omega_{fg} \simeq \Delta_t, \Omega_{res}^{(1)}) \sim (\epsilon_x'^2 + \epsilon_y'^2) \epsilon_z^2, (17)$$

which may serve for a verification of the previously discussed orbital occupancy both in the initial and the excited states.

The RIXS $d-d$ transitions to the states of higher-energy terms $(S_f \Gamma_f) \neq {}^3A_2$ listed in Fig.1 can be measured via the resonance processes that occur as $\hbar\omega_{\mathbf{k}} \rightarrow \Omega_{res}^{(n)}$, with $n > 1$. Contrary to the lowest resonance, $n = 1$, now the process $|t^2, ({}^3E)M_g e_g\rangle \rightarrow |t^2, (S_f \Gamma_f)M_f \gamma_f\rangle$ branches off, meaning that for given $n(> 1)$ there are several accessible final terms $(S_f \Gamma_f)$. Theoretically, the intertwined transitions involved could be unraveled provided the relative energy positions of the resonance energies $\Omega_{res}^{(n)}$ and the explicit form of intermediate core-hole states $\Gamma_J \gamma_J \in (n)$ are found, which would again require using computer codes. Although the overall inspection of the RIXS processes is not given herein, nevertheless a valuable piece of information regarding the expected RIXS spectra is predicted, as presented in Fig.1 together with complementary estimates in Section II, and the lowest $d-d$ excitation is studied in great detail.

So far, when classifying the multiplets of the t^2 configurations based on the symmetry-group technique, we assumed that in high- T phase a deviation from the D_{4h} symmetry is too weak to be resolved experimentally. With decreasing temperature, one expects that the deviation increases and the experimental resolution permits the main effects of the symmetry reduction $D_{4h} \rightarrow D_{2h}$ to be observed in RIXS spectra. Although, a reduction of the former multiplet structure of t_{2g}^2 configuration to a new one due to the local symmetry lowering is a routine theoretical procedure, a precise analysis of the expected *fine* structure of RIXS spectra at low temperatures is further complicated by the spin-orbital ordering. Actually, since in the lattice the neighboring V ions are now coupled by the inter-site spin-orbital superexchange, the states of a local multiplet are split by internal exchange fields and the former degeneracy is removed. In particular, the symmetry breaking of the ground-state multiplet 3E gives rise to a number of low-energy spin/orbital excitations whose energy position (and dispersion properties) are set by the superexchange constant $J \sim 10\text{meV}$, and hence the excitations are expected^{3,31-33} well below 0.1eV . From the perspective of RIXS measurements, the energy region of interest, $\hbar\omega_{fg} < 0.1\text{eV}$, is typically submerged by the tail of the huge elastic peak, which makes the selection of the lowest spectral features a problematic procedure.

In this respect, the promising dispersive quasiparticles for the RIXS measurement originate from the $d-d$ excitations thus far regarded to be localized excitons, i.e., the bound electron-hole pairs in the valence t_{2g} subshell of V ion. A mechanism behind the exciton delocalization is very similar to that proposed for the orbital wave propagation.⁶ It involves a simultaneous exchange of two *active* t_{2g} orbitals at neighboring V-V pairs forming three distinguished bonds along lattice axes. For instance, since in the lowest $d-d$ excitation of 3A_2 symmetry the d_ζ orbital involved is *inactive* along $z||\mathbf{c}$ axis, the dispersion law of the corresponding exciton is of pure two-dimensional form: $E(\mathbf{q}) = E_0 + (W/4)(\cos q_x + \cos q_y)$. Here, rough estimate for the bandwidth is $W = \alpha W'$, where $W' \sim 50\text{meV}$ and the parameter $\alpha (< 1)$ takes into account the temperature dependent spin and orbital intersite correlations in different phases. The excitonic gap E_0 is determined by the t_{2g} orbital CF splitting $\tilde{\Delta}_t$ renormalized compared to Δ_t due to intersite superexchange coupling. In disordered high- T phase of RVO_3 , one has $E_0 = \Delta_t$, assuming that a small self-energy correction due to virtual intersite t_{2g}^2 -electron hoppings is already included into Δ_t that should be measured. We conclude this short discussion with a general remark that much more work is needed to dis-

criminate all possible delocalization mechanisms responsible for a formation of propagating excitonic states. It seems that a further improvement of the experimental RIXS resolution towards the 10 meV level is required to measure these quasiparticles.

VI. CONCLUSION

To summarize, we developed the RIXS theory and applied it to predict most prominent features of the low-energy $d-d$ excitations that can be measured in RVO_3 - a prototypical Mott-Hubbard insulator with t_{2g}^2 configuration of V^{3+} ions. Complementary *ab initio* cluster calculations allowed us to estimate the crystal field parameters and choose a proper basis set for vanadium $3d$ orbitals. Initial (ground), intermediate, and final states accessible in RIXS processes were classified with the use of the symmetry-group technique, which is prerequisite to the subsequent analysis developed. To go beyond the fast collision approximation frequently used for calculations of the RIXS transition amplitude, we examined the intermediate core-hole states, including the spectral and symmetry properties of many-electron wavefunctions, with more detail than usually done before. Eventually, the problem of deducing a detailed overall picture for the intermediate states was reduced to a diagonalization of a local Hamiltonian which involves the valence electron $d-d$ and the core-hole-valence $p-d$ interactions. Mostly because of the huge number of many-body core-hole states entangled, the diagonalization procedure is far from being a trivial one. As well known, such a difficulty one encounters in any theoretical analysis of XAS spectra³⁴ in strongly correlated electron systems, which requires using specially designed computer codes. At this stage, we avoided doing any numerical calculations, but instead pursued an analytical treatment so far as possible and found, for instance, that a comprehensive analysis of the lowest $d-d$ excitations is attainable in a simple fashion. For the basic t_{2g}^2 configuration, the relative spectral position of $d-d$ excitations of higher energy is predicted and expressed in terms of a model Hamiltonian describing the local electronic properties of RVO_3 . In the present study we restrict ourselves to the calculation of RIXS spectra expected in a spin- and orbital-disordered high- T phase of RVO_3 . An extension to ordered phases, which is only shortly discussed, may be a subject of a further work. Delocalization of low-energy $d-d$ excitations leading to a formation of propagating excitonic states was also discussed and some predictions were formulated. Along this way, a future careful theoretical study and subsequent

examination by RIXS of low-energy excitations in RVO_3 will provide a better understanding of the microscopic mechanisms responsible for rich properties observed in this promising system.

To conclude, we believe that the suggested theoretical approach may be extended and applied to a description of selective RIXS transitions in other transition metal oxides with partially filled t_{2g} orbitals. In further perspective, the *ab initio* quantum-chemical cluster approach can be also applied first to calculate multiplet structure of both the ground-state t_{2g}^N and the core-hole $t_{2g}^{N+1}\underline{p}$ configurations and, second, to evaluate the matrix elements of the dipole transition operator between them. In this context, a symmetry group analysis developed here for a particular case of V^{3+} can be immediately developed to provide a complementary tool for classifying the calculated many-electron wavefunctions and controlling the symmetry selections of different $d-d$ transitions.

VII. ACKNOWLEDGMENTS

We thank J. van den Brink, M. Grüninger, P. Fulde, and L. H. Tjeng for useful discussions. One of the authors (V.Yu.) acknowledges partial financial support from the Heisenberg-Landau program.

References

- ¹ L. Ament, M. van Veenendaal, T. P. Devereaux, J. P. Hill, and J. van den Brink, *Rev. Mod. Phys.* **83**, 705 (2011)
- ² S. Miyasaka, Y. Okimoto, M. Iwama, and Y. Tokura, *Phys. Rev. B* **68**, 100406 (2003)
- ³ S. Miyasaka, J. Fujioka, M. Iwama, Y. Okimoto, and Y. Tokura, *Phys. Rev. B* **73**, 224436 (2006)
- ⁴ M. Reehuis, C. Ulrich, P. Pattison, B. Ouladdiaf, M. C. Rheinstadter, M. Ohl, L. P. Regnault, M. Miyasaka, Y. Tokura, and B. Keimer, *Phys. Rev. B* **73**, 094440 (2006)
- ⁵ A.M. Oleś et.al., *Phys. Rev. B* **72**, 214431 (2005)
- ⁶ A.M. Oleś, P. Horsch, and G. Khaliullin, *Phys. Rev. B* **75**, 184434 (2007)
- ⁷ P. Horsch, A. M. Oles, L. F. Feiner, and G. Khaliullin, *Phys. Rev. Lett.* **100**, 167205 (2008)
- ⁸ A.M. Oleś, *J. Phys.: Condens. Matter* **24**, 313201 (2012)
- ⁹ M. Reehuis, C. Ulrich, K. Prokes, S. Mat’as, J. Fujioka, S. Miyasaka, Y. Tokura, and B. Keimer, *Phys. Rev. B* **83**, 064404 (2011)
- ¹⁰ J. S. Griffith, *The Theory of Transition Metal Ions*, (Cambridge University Press, Cambridge, 1971).
- ¹¹ L. Hozoi and P. Fulde, in *Computational Methods for Large Systems: Electronic Structure Approaches for Biotechnology and Nanotechnology*, edited by J. R. Reimers (John Wiley and Sons, Hoboken, 2011), Chap. 6.
- ¹² H.-J. Werner, P. J. Knowles, G. Knizia, F. R. Manby, M. Schutz et al., molpro 2010, see [<http://www.molpro.net>]
- ¹³ L. Siurakshina, B. Paulus, V. Yushankhai, and E. Sivachenko, *Eur. Phys. J. B* **74**, 53 (2010)
- ¹⁴ G. R. Blake, A. A. Nugroho, M. J. Gutmann, and T. T. M. Palstra *Phys. Rev. B* **79**, 045101 (2009)
- ¹⁵ J.-S. Zhou and J. B. Goodenough, *Phys. Rev. B* **77**, 132104 (2008)
- ¹⁶ M. De Raychaudhury, E. Pavarini, and O. K. Andersen, *Phys. Rev. Lett.* **99**, 126402 (2007)
- ¹⁷ T. Mizokawa and A. Fujimori, *Phys. Rev. B* **54**, 5368 (1996)

- ¹⁸ E. Bencksier, R. Rückamp, T. Möller, T. Taetz, A. Möller, A. A. Nugroho, T. T. M. Palstra, G. S. Uhrig, and M. Grüniger, *New J. Phys.* **10**, 053027 (2008)
- ¹⁹ D.M. Pease, *Phys. Rev. B* **44**, 6708 (1991)
- ²⁰ M.O. Krause, and J.H. Oliver, *J. Phys. Chem. Ref. Data* **8**, 329 (1979)
- ²¹ M. van Veenendaal, P. Carra, and B. T. Thole, *Phys. Rev. B* **54**, 16010 (1996)
- ²² J. van den Brink and M. van Veenendaal, *Europhys. Lett.* **73**, 121 (2006)
- ²³ M. van Veenendaal, *Phys. Rev. Lett.*, **96**, 117404 (2006)
- ²⁴ G. van der Laan, B. T. Thole, G. A. Sawatzky, and M. Verdagner, *Phys. Rev. B* **37**, 6587 (1988)
- ²⁵ F. M. F. de Groot, J. C. Fuggle, B. T. Thole, and G. A. Sawatzky, *Phys. Rev. B* **42**, 5459 (1990).
- ²⁶ H. Ikeno, F.M.F. de Groot, E. Stavitski, and I. Tanaka, *J. Phys.: Condens. Matter* **21**, 104208 (2009)
- ²⁷ E. Stavitski, and F.M.F. de Groot, *Micron* **41**, 687 (2010)
- ²⁸ A. Uldry, F. Vernay, and B. Delley, *Phys. Rev. B* **85**, 125133 (2012)
- ²⁹ M. Haverkort, <http://arxiv.org/abs/cond-mat/0505214>
- ³⁰ G.F. Koster, J.O. Dimmock, R.G. Wheeler, and H. Statz, *Properties of the thirty-two Point Groups*, (M.I.T. Press, Cambridge, Massachusetts, 1963)
- ³¹ S. Ishihara, *Phys. Rev. B* **69**, 075118 (2004)
- ³² S. Sugai and K. Hirota, *Phys. Rev. B* **73**, 020409(R) (2006)
- ³³ S. Jandl, A.A. Nugroho, and T.T.M. Palstra, *J. Phys.: Conf.Series* **200**, 032025 (2010)
- ³⁴ G. van der Laan, *Hitchhiker's Guide to Multiplet Calculations*, in *Lect. Notes Phys.* **697**, 143 (2006)

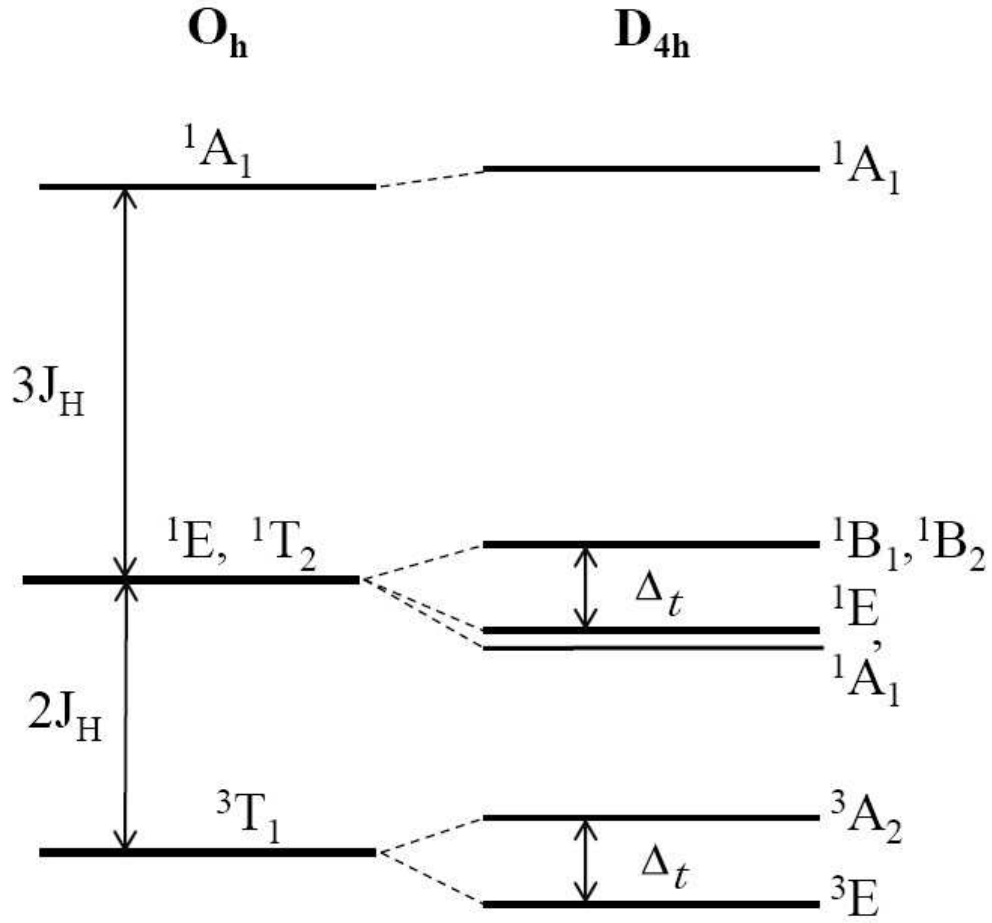


FIG. 1: Multiplet structure of t_{2g}^2 configuration of V^{3+} ion in crystal field of D_{4h} symmetry. The term branching with the symmetry reduction $O_h \rightarrow D_{4h}$ is shown for clarity. In RIXS the initial (ground) state is given by 3E and other terms correspond to local $d-d$ excitations. More precise estimates for the excitation energies are given in the text.